www.ietdl.org

Published in IET Signal Processing
Received on 6th December 2012
Revised on 30th July 2013
Accepted on 19th October 2013
doi: 10.1049/iet-spr.2012.0384

ISSN 1751-9675

Error probability upper bound for perfect sequences implemented with super-structured fibre Bragg gratings

João S. Pereira[1,2], *Henrique J.A. da Silva*[2]

[1]*DEI/ESTG, Instituto Politécnico de Leiria, Alto do Vieiro, Morro do Lena, P-2401-951 Leiria, Portugal*
[2]*Instituto de Telecomunicações, Universidade de Coimbra, Polo II, P-3030-290 Coimbra, Portugal*
E-mail: joao.pereira@ipleiria.pt

Abstract: The success of coherent optical code-division multiple-access (OCDMA) systems is strongly dependent on the optical encoder/decoder technology and on the selection of the correct OCDMA codes/sequences. For this reason, in this study, the authors present a method to implement perfect sequences with Super-Structured Fibre Bragg Gratings (SSFBGs). A new SSFBG power reflection model has been found. They have also derived a property that explains why the SSFBGs should use codes derived from *m*-sequences. Usually, OCDMA researchers try many different codes into SSFBGs in order to select the SSFBG encoders that result in lower error probability. In the authors work, they show that a SSFBG can be considered to be a perfect sequence encoder. For this reason, the codes written into the SSFBGs should be selected based on their new property. This property permits to design and select quickly the correct codes with low power contrast ratios. In addition, a new error probability upper bound, which is a function of the code family and of its power contrast ratio is also presented. With this new bound, it is not necessary to use an optical simulator to estimate the maximum bit error rate of an OCDMA system, if some power contrast ratios of the selected SSFBG code set are known.

1 Introduction

Nowadays, two standards are under massive deployment around the world: Ethernet Passive Optical Network (EPON) (IEEE 802.3ah) and Gigabit capable Passive Optical Network (GPON) (ITU-T G.984). Such standards [1] provide high throughputs to the customers over a single mode fibre, reaching 20 km and use the time-division multiplexing (TDM) technique.

Other techniques, such as wavelength-division multiplexing (WDM), are under investigation for application in Passive Optical Network (PON). The next PON generation can be either 10G-EPON (IEEE 802.3av) or NG-PON (next generation PON), based on WDM. However, coherent optical code-division multiple-access (OCDMA) is also an efficient alternative to TDM and WDM techniques.

Around 1990, some experiments demonstrated encoding and decoding of femtosecond pulses, and suggested the possibility of ultrahigh speed code-division multiple-access (CDMA) communications [2]. Previous reports on the use of optical CDMA (OCDMA) can be found in [3, 4].

OCDMA, where different codes are assigned to different users during transmission, is a promising candidate for next-generation broad-band access networks. The Super-Structured Fibre Bragg Grating (SSFBG) [5] may be used as a coherent optical encoder that offers high performance, compactness, compatibility with the fibre-optic system and potentially low cost, making it an attractive choice for coherent time spreading (TS) OCDMA encoding/decoding [6, 7]. The OCDMA PON concept offers several unique advantages [8–13]. An OCDMA network can implement a fully asynchronous transmission without requiring complex and expensive electronic equipment and protocols. This process can guarantee a low-delay access because coding operations are performed all optically and passively. Another advantage is the soft capacity increase that allows adding users as demand increases. OCDMA-PON has a high potential of security provided by the use of long pseudorandom codes for transmission. OCDMA-PON provides control of the quality of service (QoS), which can be easily guaranteed in the physical layer by assigning different codes based on the QoS required by each user. In summary, coherent TS-OCDMA-PON is experiencing a renewed interest because of its promise of high levels of security at ultra-high data rates, simplified network control and support for asynchronous burst communications [14]. However, the required mode-locked laser (MLL) sources remain costly. This major problem should be minimised after MLL mass production. Other compact and reliable devices that may be used as OCDMA encoder/decoders (CODECs), besides the SSFBG, are planar lightwave circuits (PLC) [15], spatial lightwave phase modulators [16] and arrayed waveguide gratings [17]. The total throughput of asynchronous coherent TS-OCDMA has reached 320 Gb/s with more than 12 active users and a spectral efficiency of 0.32 b/s/Hz [18].

A ten-users truly asynchronous gigabit coherent OCDMA system has also been experimentally demonstrated without using any timing coordination [19]. This technique has been developed to support 640 Gchip/s over 50 km in a coherent OCDMA-PON, using long Gold codes [20] with 511 chips.

SSFBGs are easily written by applying a spatial variation pattern of ultraviolet light to the core of a short section of optical fibre with a few millimetres length. For this reason, we have focused our attention on this type of low-cost OCDMA CODECs. More specifically, we have selected and evaluated the SSFBG presented in [5]. Usually, the codes written in SSFBGs are selected based on a low power contrast ratio (*P/C*). Therefore the best selected codes are often some bipolar codes of Gold sets. It is well known that the correlation properties of these codes (derived from maximum length sequences) are very good. However, only a few Gold codes are adequate for SSFBGs [20] and are dependent of the ultraviolet light writing precision.

In Section 2, we introduce a generic model for a coherent OCDMA system. Section 3 presents a new OCDMA error probability upper bound as a function of the power contrast ratio *P/C* of the code family selected. The following Section 4 shows that SSFBGs can implement perfect sequences. A new SSFBG power reflection model has been found and a property is presented to explain why the SSFBG should use codes derived from Gold codes or *m*-sequences. Some simulation experiments using Optiwave® software are described in Section 5, and the main conclusions are gathered in the last section.

2 Coherent OCDMA sistema

In coherent TS-OCDMA, the coherence of the optical signal has to be maintained within the chip duration, and so the coherent beat noise becomes critical. We have examined the beat noise, along with multiple-access-interference (MAI) and receiver noise, and the effects of such noise sources on incoherent, coherent and partially coherent TS-OCDMA. In coherent TS-OCDMA (e.g. with PLC or SSFBG), the coherence of light τ_c should be maintained at least within each chip duration T_c; that is, $\tau_c \geq T_c$.

The beat noise issue has been studied with respect to spectral coding OCDMA systems [21, 22] and two-dimensional (2D) OCDMA [23].

For a TS-OCDMA network employing chip-rate square-law photodetection, the signal at the integrator output is

$$Z \simeq T_c \Re(P_d) + T_c \Re\left(\sum_{i=1}^{K-1} \mathrm{P}_i\right) + T_c \Re\left(2\sum_{i=1}^{K-1}\sqrt{P_i P_d}\cos(\Delta\varphi_i)\right) + \int_0^{T_c} n_0(t)\,\mathrm{d}t \quad (1)$$

where $\Re$ is the responsivity of the photodetector, P_d is the optical intensity of the signal decoded for the targeted user, P_i is the signal received for an untargeted user (interferer), $\Delta\varphi_i$ is a random process that varies over $[-\pi, +\pi]$ from bit to bit (which is the beat noise of a coherent TS-OCDMA system), and n_0 denotes the receiver noise current. We assume that there are K active users transmitting asynchronously in the network. This means that there are $K-1$ interfering signals from untargeted active users at a given instant.

In (1), the first term $T_c\Re(P_d)$ is the target signal, the second term $T_c\Re\left(\sum_{i=1}^{K-1} P_i\right)$ represents the MAI noise, the third term

$$T_c \Re\left(2\sum_{i=1}^{K-1}\sqrt{P_i P_d}\cos(\Delta\varphi_i)\right)$$

is the primary data-interference beat noise, and the final term $\int_0^{T_c} n_0(t)\,\mathrm{d}t$ represents the receiver noise. Here, the polarisation states of the data and interfering signals are assumed to be the same (the worst-case scenario) and the secondary data-interference beat noise has been omitted (when K is not very large, such that $K-1 \ll \sqrt{(\langle P_d\rangle)/(\langle P_i\rangle)}$, the secondary beat noise can be ignored). $\xi \equiv ((\langle P_i\rangle)/(P_d))$ is the crosstalk level and $\langle\rangle$ represents the ensemble average. Usually, in a TS-OCDMA-PON, the crosstalk level ξ is very small. For example, in a coherent TS-CDMA-PON employing SSFBGs written with Gold codes [24] or $P(y, x)$ codes of length N [25], $\xi \simeq (1/N)$.

3 OCDMA error probability

For the estimation of error probability, an asynchronous TS-OCDMA communication system is similar to an asynchronous DS-CDMA (direct-sequence code division multiple access) wireless communication system with a BPSK (binary phase shift keying) modulation. For both communication systems, the average error probability P_e is approximately equal to [26–28]

$$P_e \simeq 1 - \phi\left[\left(\frac{N_0}{2E_b} + \frac{1}{6N^3}\sum_{\substack{k=1\\k\neq i}}^{K} r_{k,i}\right)^{-1/2}\right] \quad (2)$$

where E_b is the bit energy, $N_0/2$ is the two-sided spectral density of an AWGN (additive white Gaussian noise) channel noise process, ϕ is the normalised (i.e. zero mean, unit variance) Gaussian cumulative distribution function, K is the number of simultaneous users and $r_{k,i}$ is a function of the aperiodic autocorrelation functions $C_{k,k}(l) = C_k(l)$ and $C_{i,i}(l) = C_i(l)$ of the codes k and i [29]

$$r_{k,i} = 2N^2 + 4\sum_{l=1}^{N-1} C_k(l)C_i(l) + \sum_{l=1-N}^{N-1} C_k(l)C_i(l+1) \quad (3)$$

An alternative expression for $r_{k,i}$ is a function of the aperiodic cross-correlation function $C_{k,i}(l)$ [26]

$$r_{k,i} = 2\sum_{l=1-N}^{N-1} C_{k,i}^2(l) + \sum_{l=1-N}^{N-1} C_{k,i}(l)C_{k,i}(l+1) \quad (4)$$

A SSFBG decoder is normally used before a photodetector device. Therefore the SSFBG output signal is an optical signal with a phase modulation. To simplify the study and analysis of the SSFBG error probability, we chose to consider only bipolar codes (with two phases: 0 and π). In this scenario, phase modulation is simply a BPSK modulation and the system to be analysed is a TS-OCDMA-PON system with coherent coding and decoding making use of bipolar codes. The error probability P_e may be used to find an upper bound for a CDMA or OCDMA system. This P_e upper bound $\max\{P_e\}$,

doi: 10.1049/iet-spr.2012.0384

when $C_{k,\,i}(l)$ is replaced by $\max\{C_{k,\,i}\}$, can be rewritten as a function of the power contrast ratio [20] $P/W = 20\log[C_k(0)/\max\{C_{k,\,k}\}]$ (in dB), using (3). However, it is preferable to rewrite the upper bound as a function of another power contrast ratio $P/C = 20\log[C_k(0)/\max\{C_{k,\,i}\}]$ (in dB), using (4). Some P/W and P/C upper bounds, for periodic correlations, have been found. One of them is the Welch bound [24] of K perfect sequences of length N: $P/C = 20\log\sqrt{((KN-1)/(K-1))}$ (P/C = 17.85 dB when $K = 2$, $N = 31$ and $P/W = \infty$). For the aperiodic correlation case, the upper bound is

$$P/C = 20\log\sqrt{\frac{2KN-K-1}{K-1}}$$

(P/C = 20.83 dB when $K = 2$ and $N = 31$).

The code set selected should have a high P/C value. For example, it has been suggested that the SSFBG should have power contrast ratios (P/W and P/C) higher than 17 dB for 127-chips Gold codes [20].

In this study, we only consider the P/C ratio, and the outputs of the OCDMA-PON decoders are normalised so that $C_k(0) = N$. Therefore the upper bound of an aperiodic cross-correlation is simple

$$\begin{aligned} &\max\{C_{k,\,i}\} = N \times 10^{-((P/C)/(20))} \\ &\text{with } \; -N+1 \le l \le N-1 \end{aligned} \tag{5}$$

Using (2), (4) and (5) we find an upper bound of the error probability as a function of the power contrast ratio P/C

$$\begin{aligned} &\max\{P_\mathrm{e}\} \\ &\simeq 1 - \phi\left[\left(\frac{N_0}{2E_\mathrm{b}} + (K-1)\left(1-\frac{1}{N}\right)10^{-((P/C)/(10))}\right)^{-1/2}\right] \end{aligned} \tag{6}$$

For this result, $C_{k,\,i}(l)$ has been replaced in (2) with the maximum value defined by (5), for any integer $-N+1 \le l \le N-1$. In other words, the upper bound (6) may be considered a worst case scenario, because the value of $C_{k,i}(l)$ has been considered equal to a maximum constant value $\max\{C_{k,\,i}\}$.

Fig. 1 shows a 3D representation of the upper bound (6), for $K = 2$ and $N = 31$. For example, the error probability upper bound is lower than 10^{-5} when the two ratios P/C and E_b/N_0 are at least equal to 15 dB. This situation requires a bit error correction method to guarantee an error free transmission. However, we should remember that (6) gives us the worst case error probability. Frequently, the error probability average defined by (2) is utilised and, of course, this average will be much lower than the worst case (6).

An alternative solution to obtain a lower BER (bit error rate) is to increase the code length. Fig. 2 shows a 3D representation of the BER upper bound when 10 users are used simultaneously with a code length equal to 511, as in [19].

The error probability upper bound (6), when 10 codes are used simultaneously, has a P/C approximately equal to $10 \times \log(N)$. That is, 27 dB when N is equal to 511 chips. This contrast ratio gives us an error probability upper bound almost equal to 10^{-13}.

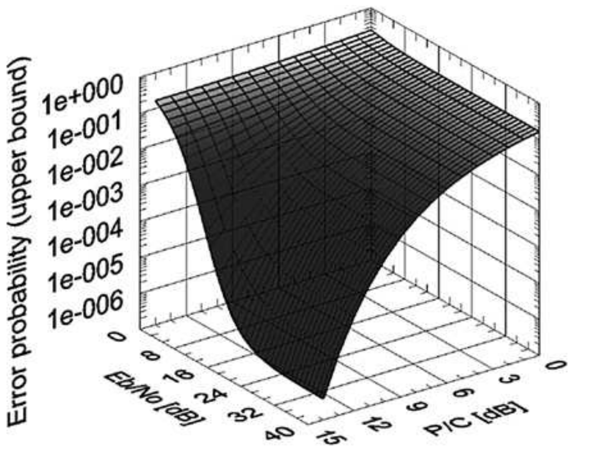

Fig. 1 *3D representation of the upper bound of the error probability defined by (6) as a function of P/C and E_b/N_0, when K = 2 and N = 31*

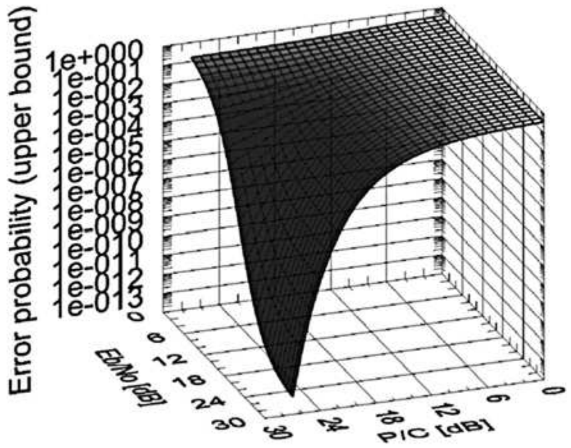

Fig. 2 *3D representation of the upper bound of the error probability defined by (6) as a function of P/C and E_b/N_0, when K = 10 and N = 511*

4 SSFBG can implement perfect sequences

Expression (6) should be useful when we want to design a TS-OCDMA-PON system with coherent optical encoders and decoders. For example, these optical CODECs can be SSFBGs. However, we should note that a SSFBG using a uniform grid with a recording format similar to a bipolar code, for a given wavelength, does not ensure that the encoded signal is a bipolar signal or a signal similar to a BPSK modulated one. After simulating the implementation of several code families with SSFBGs, we found that only the SSFBGs written with codes derived from Gold codes or maximum length sequences (m-sequences) exhibited good performance. The following analysis should be useful to identify the conditions required to keep the good correlation properties of the selected codes. We present a new simplified SSFBG power reflection model that enables to determine if the selected codes retain their power contrast ratios (P/W or P/C) after the recording process. Actually, not all codes of a set of Gold codes may be used in SSFBGs. Signals encoded with SSFBGs have been used by us in assessing the error probability (2) or the upper bound of the error probability (6).

The SSFBG power reflection (for a chip written over a length L) [5], is given by the following equation

$$r = \left| \frac{-\kappa \sinh\left(\sqrt{\kappa^2 - \hat{\sigma}^2} L\right)}{\hat{\sigma} \sinh\left(\sqrt{\kappa^2 - \hat{\sigma}^2} L\right) + \mathrm{j}\sqrt{\kappa^2 - \hat{\sigma}^2} \cosh\left(\sqrt{\kappa^2 - \hat{\sigma}^2} L\right)} \right|^2 \tag{7}$$

with

$$\hat{\sigma} = \left(\frac{\lambda_{\max}}{\lambda} - 1\right) \pi \frac{N_G}{L}$$

here $\lambda_{\max}$ is the wavelength of maximum reflectivity, that occurs when $\hat{\sigma} = 0$ and is given by

$$\lambda_{\max} = \left(1 + \frac{\overline{\delta n}_{\text{eff}}}{n_{\text{eff}}}\right) \lambda_D$$

To simplify the study of SSFBGs, it is possible to consider that $\lambda_{\max} \simeq \lambda_D$. Here λ is the wavelength and λ_D is the 'design wavelength' [5] for Bragg scattering by an infinitesimally weak grating. n_{eff} is the refractive index. For a single-mode Bragg reflection with a uniform grating, the 'DC' index change [5] spatially averaged over a grating period $\overline{\delta n}_{\text{eff}}$ is constant. Therefore the coefficients $\hat{\sigma}$ and κ are also constants. κ is the 'AC' coupling coefficient and $\hat{\sigma}$ is a general 'DC' self-coupling coefficient used in the coupled-mode theory of uniform gratings, where N_G is the total number of grating periods [5].

Fig. 3 shows a schematic of the physical structure of a specific SSFBG, where the separation between two chips is Δz_0 and the N sections of length L are written using the wavelength $\lambda_i = \lambda_D + i\Delta\lambda$. Where $\Delta\lambda$ is a small incremental value of the wavelength $(\Delta\lambda \ll \lambda_D)$. Each section of the grid represents a SSFBG chip etched with a phase ϕ_i.

For our SSFBG study (based on a selected family of codes) we considered that $\Delta z_0 \geq L$. The power reflection (7) can be rewritten using a Taylor series for sinh() and cosh() when $\sqrt{\kappa^2 - \hat{\sigma}^2} L$ assumes a low value. Thus, the power reflection of the first chip has been derived and it is approximately

$$r_{\text{chip}}(\lambda) \simeq \left| \frac{-\kappa_1 L}{\pi((N_G)/L)(((\lambda_{\max})/\lambda) - 1) + \mathrm{j}} \right|^2 \tag{8}$$

This expression is similar to the transfer function of a bandpass filter (BPF) centred on the wavelength $\lambda_{\max}$, with

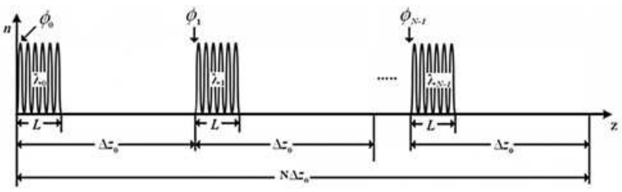

Fig. 3 *Encoder structure used to discover the power reflection as a function of a selected SSFBG code family*

the amplitude $r_{\text{chip}}(\lambda_{\max}) = |\kappa_1 L|^2$ and

$$r_{\text{chip}}(\pm\infty) = \frac{|\kappa_1 L|^2}{1 + (\pi((N_G)/L))^2} = \varepsilon |\kappa_1 L|^2 \tag{9}$$

when $\pi N_G \gg L$, then $r_{\text{chip}}(\lambda_{\max}) \gg r_{\text{chip}}(\pm\infty)$ (because $\varepsilon \ll 1$) and therefore it is possible to associate a specific SSFBG to a BPF filter.

In this scenario, it is considered that the N chips are written with the wavelengths $\lambda_i = \lambda_D + i\Delta\lambda$, for $0 \leq i \leq N - 1$, and all chips will have the same value $\kappa = \kappa_1$. For convenience, the transfer function of the first chip of the SSFBG, when $\phi_0 = 0$, may be modelled as a scaled version of the rectangular function defined by the following expression

$$\text{Rect}_\varepsilon\left(\frac{\lambda - \lambda_{\max}}{B}\right) = \begin{cases} 1 \text{ when } \lambda_{\max} - \frac{B}{2} \leq \lambda \leq \lambda_{\max} + \frac{B}{2} \\ \varepsilon \text{ other } \lambda \end{cases} \tag{10}$$

This special rectangular function, centred at $\lambda_{\max}$, has a bandwidth equal to B and a minimum amplitude equal to

$$\varepsilon = \frac{1}{1 + (\pi((N_G)/L))^2}$$

when $\pi N_G \gg L$, then $B \simeq ((2L)/(\pi N_G))\lambda_{\max}$, and (10) is cut -3 dB at $\lambda = \lambda_{\max} \pm (B/2)$. Each grid of each SSFBG chip i acts as a specific BPF with a transfer function approximately equal to the following expression

$$|\kappa_1 L|^2 \times \exp\{\mathrm{j}\phi_i\} \times \text{Rect}_\varepsilon\left(\frac{\lambda - \lambda_D - i\Delta\lambda}{B}\right) \tag{11}$$

It was considered that $\lambda_{\max} \simeq \lambda_D$. The phase ϕ_i of the chip i is shown in Fig. 3. The power reflection of a series of N chips (a train of N FBGs) is given by

$$\prod_{i=1}^{N} |\kappa_1 L|^2 \times \exp\{\mathrm{j}\phi_i\} \times \text{Rect}_\varepsilon\left(\frac{\lambda - \lambda_D - i\Delta\lambda}{B}\right) \tag{12}$$

Considering the special case when $(B/2) < \Delta\lambda < B$, then the previous expression may be considered approximately equal to

$$\sum_{i=0}^{N-1} A^2 \times \exp\{\mathrm{j}(\phi_i + \phi_{i+1})\} \times \text{Rect}_{\varepsilon_2}\left(\frac{\lambda - \lambda_D - i\Delta\lambda - ((\Delta\lambda)/2)}{W}\right) \tag{13}$$

with $A^2 = \varepsilon^{N-2}|\kappa_1 L|^4$ and $\varepsilon_2 = ((\varepsilon)/(|\kappa_1 L|^2))$.

This result (13) is obtained when the product of two consecutive rectangular functions (of index i and index $i+1$) is equal to a rectangular function with a bandwidth $W = B - \Delta\lambda$, with $0 < W < B$, centred at $\lambda_D + i\Delta\lambda + ((\Delta\lambda)/2)$. In this process, $\varepsilon_2 = ((\varepsilon)/|\kappa_1 L|^2))$ can be disregarded if (13) is sampled at the centres of rectangular pulses

$$\text{Rect}_{\varepsilon_2}\left(\frac{\lambda - \lambda_D - i\Delta\lambda - ((\Delta\lambda)/2)}{W}\right)$$

doi: 10.1049/iet-spr.2012.0384

The sampling process is equivalent to considering that the bandwidth W is reduced to an infinitesimal value. This operation will convert (13) in a function approximately equal to a train of unit pulses. That is, the SSFBG power reflection of N chips (uniformly distributed as shown in Fig. 3) is approximately equal to (13) after the sampling procedure defined by

$$\sum_{i=0}^{N-1} A^2 \times \exp\{j(\phi_i + \phi_{i+1})\} \times \delta\left(\lambda - \lambda_D - i\Delta\lambda - \frac{\Delta\lambda}{2}\right) \tag{14}$$

The function $\delta()$ is a unitary pulse. For convenience, it is considered that $\phi_N = \phi_0$. In other words, the power reflection has undergone a translation of one cycle. This simplification can be made if the codes written in SSFBGs are considered long ($N \gg 2$). In this case, the IDFT (inverse discrete Fourier transform) of a normalised SSFBG power reflection (IDFT of (14) around $\lambda_D + ((\Delta\lambda)/2)$), is approximately proportional to the following expression

$$x_{\mathrm{SSFBG}}(n) \propto \sqrt{N} \times \mathrm{IDFT} \left\{ \sum_{i=0}^{N-1} \exp[j(\phi_i + \phi_{i+1})] \times \delta(\lambda - i\Delta\lambda) \right\} \tag{15}$$

when the input of the SSFBG is a unitary pulse with an amplitude $((\sqrt{N})/(A^2))$. After the $\lambda_D + ((\Delta\lambda)/2)$ translation of (14), this signal (15) can be considered as a baseband signal, which should be useful in determining the power contrast ratios P/W and P/C of the codes written in the SSFBG.

Each chip i of a SSFBG, when $(B/2) < \Delta\lambda < B$, has a phase $\theta_i = \phi_i + \phi_{i+1}$ and an amplitude which is equal to a constant for all chips. This means that the SSFBG power reflection baseband signal, defined by the model (15), is the IDFT of a unimodular sequence. Obviously, (15) is a perfect sequence. Before proceeding with the analysis of these perfect sequences, for SSFBGs written with some code families, it is necessary to consider that the periodic autocorrelation function should be a good estimator of an aperiodic autocorrelation function (when the code is long).

Now, we should remember that SSFBGs are usually written with bipolar m-sequences or a subset of bipolar Gold codes (with two phases 0 and π). For this reason, we should verify some correlation properties of these codes when the phase is $\theta_i = \phi_i + \phi_{i+1}$. For example, the power contrast ratio P/C must be investigated to ensure that the condition $(B/2) < \Delta\lambda < B$ will not compromise the correlation properties of the codes written in the SSFBG. Using one of the properties of [27] or [28], the power contrast ratio P/C of Gold codes (excluding one of the two m-sequences of the Gold set) is found to be approximately equal to

$$P/C \simeq 20\log\left(\frac{N}{\sqrt{N+1}}\right) \tag{16}$$

if the codes written in SSFBG are bipolar Gold codes $m_r = \chi(u \oplus T^r v)$, with length N and phase ϕ_i. The sequence m_r is derived from two m-sequences u and v. These sequences u and v are 'preferred pairs' of m-sequences. T^r denotes the operator which shifts sequences cyclically to the left by r places: $T^r z = (z(r), z(r+1), \ldots, z(N-1), z(0), \ldots, z(r-1))$.

The $\oplus$ operator is used to denote modulo-2 addition (or the EXCLUSIVE-OR operation). The function $\chi(.)$ is defined by $\chi(0) = +1$ and $\chi(1) = -1$. These codes were previously presented in [27].

A code with the SSFBG phase $\theta_i = \phi_i + \phi_{i+1}$ is equivalent to the code $m_r T^1(m_r)$. This conclusion is simple to verify if (15) is rewritten as

$$x_{\mathrm{SSFBG}}(n) \propto \sqrt{N} \times \mathrm{IDFT} \left\{ \begin{array}{l} \left(\sum_{i=0}^{N-1} \exp[j(\phi_i)] \times \delta(\lambda - i\Delta\lambda) \right) \\ \quad \times \sum_{i=0}^{N-1} \exp[j(\phi_{i+1})] \times \delta(\lambda - i\Delta\lambda) \end{array} \right\} \tag{17}$$

with

$$m_r = \sum_{i=0}^{N-1} \exp[j(\phi_i)] \times \delta(\lambda - i\Delta\lambda)$$

and

$$T^1(m_r) = \sum_{i=0}^{N-1} \exp[j(\phi_{i+1})] \times \delta(\lambda - i\Delta\lambda)$$

considering $\phi_N = \phi_0$.

Consequently, the value (16) may be derived based on the following property:

Property: The maximum absolute value of periodic cross-correlation between two perfect sequences

$$y = \sqrt{N} \times \mathrm{IDFT}[m_r T^1(m_r)]$$

and

$$z = \sqrt{N} \times \mathrm{IDFT}\left[m_q T^1(m_q)\right]$$

when $r \neq q$, with $-1 \leq r, q \leq N-1$, where r, q are integers, is $\max\{|\theta_{yz}|\} = \sqrt{N+1}$, when $m_r = \chi(u \oplus T^r v)$, $T^1 m_q = \chi(T^1 u \oplus T^{q+1} v)$ and u, v are m-sequences.

Some steps of the proof of this property can be found in [27] or [28]. For example, the sequences

$$y = \sqrt{N} \times \mathrm{IDFT}[m_r T^1(m_r)]$$

and

$$z = \sqrt{N} \times \mathrm{IDFT}\left[m_q T^1(m_q)\right]$$

are perfect sequences because $|\chi(u \oplus T^r v)\chi(T^1 u \oplus T^{r+1} v)| = 1$ and $|\chi(u \oplus T^q v)\chi(T^1 u \oplus T^{q+1} v)| = 1$. Finally, the absolute periodic cross-correlation value can be written as

$$\begin{aligned} \left|\theta_{yz}(n)\right| &= |N \times \mathrm{IDFT}\{\chi(u)\chi(T^r v)\chi(T^1 u)\chi(T^{r+1} v) \\ &\quad \times [\chi(u)\chi(T^q v)\chi(T^1 u)\chi(T^{q+1} v)]^*\}| \\ &= |N \times \mathrm{IDFT}[\chi(T^p v)\chi(T^{p+1} v)]| \\ &= |N \times \mathrm{IDFT}[\chi(T^k v)]| \end{aligned} \tag{18}$$

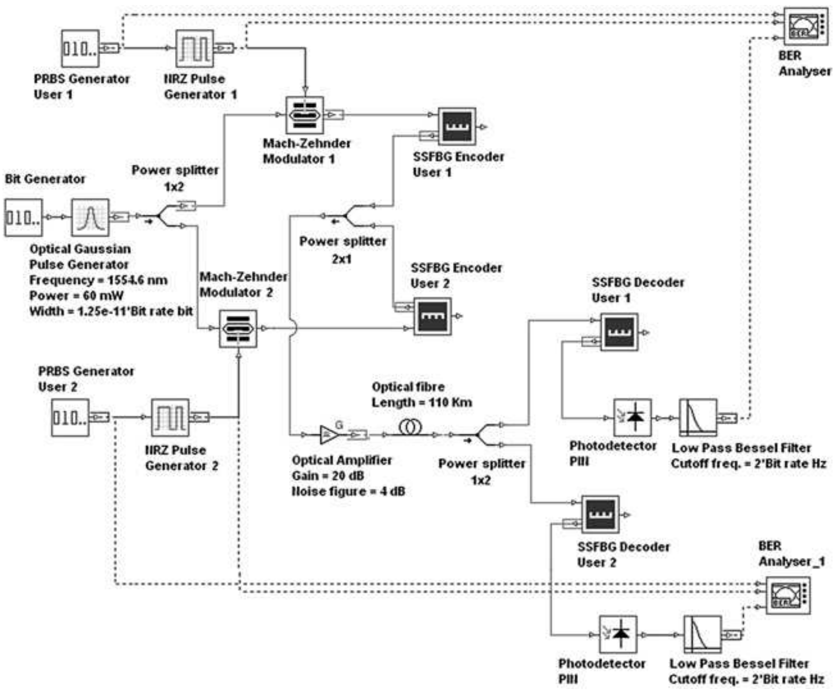

Fig. 4 *Two users OCDMA-PON scenario implemented with Optiwave® simulator (two SSFBGs written with two Gold codes, when N = 31)*

here the operator T^k can be dropped and we find that

$$\max\left\{\left|\theta_{yz}\right|\right\} = \max\left\{\left|\pm\sqrt{N+1-N\delta(n)}\right|\right\} = \sqrt{N+1}$$

when $(B/2) < \Delta\lambda < B$, it is necessary to use the previous property. However, when $\Delta\lambda \geq B$ then $\theta_i = \phi_i$, $A^2 = \varepsilon^{N-1}/\kappa_1 L/^2$ and $\varepsilon_2 = ((\varepsilon)/(/\kappa_1 L/))^2$. In both cases, we obtain

$$P/C \simeq 20\log\left(\frac{N}{\sqrt{N+1}}\right)$$

with the models (15) and (17).

Unfortunately, when $\Delta\lambda \leq (B/2)$, (14) is not valid. Therefore the models (15) and (17) can no longer be used when $\Delta\lambda \leq (B/2)$.

Usually, researchers try many different codes into SSFBGs and select the SSFBG encoders with the best BER results. In addition, longer codes are better than short codes and can be used to improve OCDMA-PON communication systems. For example, in [19], the authors have used SSFBGs written with Gold codes of 511 chips to avoid the effect of low power contrast ratios and the harmful beat noise. In our work, we show that a SSFBG can be considered a perfect sequence encoder and the codes written into the SSFBG should be influenced by the new 'Property' presented above. This 'Property' shows that Gold codes or maximum length code families can be used into the SSFBG encoders. However, this 'Property' reveals us that not all Gold codes of the same Gold set, with the same length, can be written into SSFBG encoders. More specifically, one of the two maximum length codes of a Gold set decreases the P/C ratio and for this reason it should be discarded of the Gold set.

5 SSFBG OCDMA simulations with Optiwave®

To confirm the validity of the upper bound presented in Fig. 1, with bipolar codes of length 31, we decided to perform an alternative simulation using the Optiwave® software. Fig. 4 represents an OCDMA-PON scenario with two asynchronous users, with 1 Gbps per user at the wavelength of 1550 nm. Each user encodes its transmission with a SSFBG written with a randomly selected Gold code of length $N = 31$.

The single mode fibre length between the SSFBG encoder and the SSFBG decoder is about 110 km. This optical link has an attenuation of 0.2 dB/km. At the entrance of the fibre, we used an optical amplifier with a gain of 20 dB. Therefore between the output of the SSFBG encoders and the SSFBG decoders entrance there exists a net loss of 2 dB. The Gold codes of length 31 which were considered have a P/C of approximately 15 dB. The signal-to-noise ratio (S/N) at the output of each SSFBG was configured much higher than this value P/C of 15 dB. In our scenario of Fig. 4, we can say that the BER depends mainly on the power contrast ratio P/C. The net loss of 2 dB affects the two ratios S/N and P/C. However, the BER will be essentially affected by the lower ratio P/C that will be 13 dB (or 15–2 dB). Using the error probability upper bound of Fig. 1, we can read a $\max\{P_e\}$ value approximately equal to 5×10^{-5} when $P/C = 13$ dB.

Fig. 5 shows the eye diagram and the minimum BER of 5.7×10^{-6} achieved in the OCDMA-PON scenario of Fig. 4 for the user 1 (SSFBG 1 user target, written with a Gold code with $N = 31$). This minimum BER value, estimated by Optiwave®, is 11 times lower than the $\max\{P_e\}$ (maximum upper bound) used by us with (6) and Fig. 1.

In our scenario, we have considered that the BER is equal to the error probability (P_e). The Optiwave® simulator gives us the minimum BER, but not the maximum BER. For this

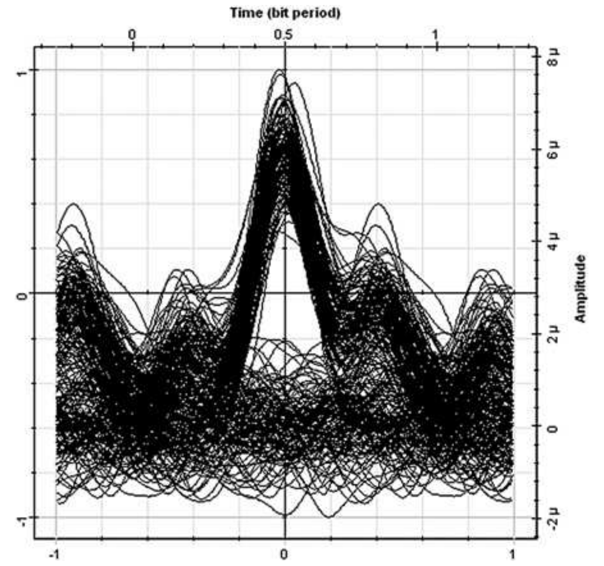

Fig. 5 *Eye diagrams achieved in OCDMA-PON scenario of Fig. 4*
(two SSFBG CODECs written with a different Gold code when $N = 31$ and a bit rate of 1 Gbps over 110 km of fibre), with the SSFBG decoder of User 1, when the minimum BER achieved is 5.7×10^{-6}

reason, we only can say that the minimum BER should be always lower than our new maximum BER (6), when the sampling operation is performed at the middle of a bit period. This situation has been verified with different SSFBG Gold codes of the scenario considered in Fig. 4. Fig. 6 presents a comparison between our new maximum BER and the minimum BER (of Optiwave®). As we can see, the minimum BER is lower than our new maximum BER when the sampling time is approximately at the middle of the bit period. More simulations have been performed with Optiwave®, using different codes and different line transmission lengths. Unfortunately, we found unpredictable fluctuations of the minimum BER around the middle of the bit period that depend of many different parameters. We can only say that, when the sampling time is approximately at the middle of the bit period, the minimum Optiwave® BER is frequently close to the new maximum BER (6) and is slightly lower, in half of the cases. Despite our small set of simulations, we are confident to say that our new maximum BER should be useful and can be an alternative when we want to estimate the BER of an OCDMA-PON communication system with coherent SSFBG encoders, without the use of an optical simulator.

We can conclude that the selection of the appropriate codes, the SSFBG ultraviolet light writing precision and the precision of the optical communication synchronisation (sampling operation) are important when we want to design a gigabit OCDMA-PON transmission system with low BER over more than 100 km. A second important conclusion is that our Optiwave® simulation results are consistent with the new error probability upper bound that has been presented in (6). Therefore it is not necessary to use an optical simulator to estimate the maximum BER of an OCDMA-PON system if the *P/C* ratios of the SSFBG codes are known.

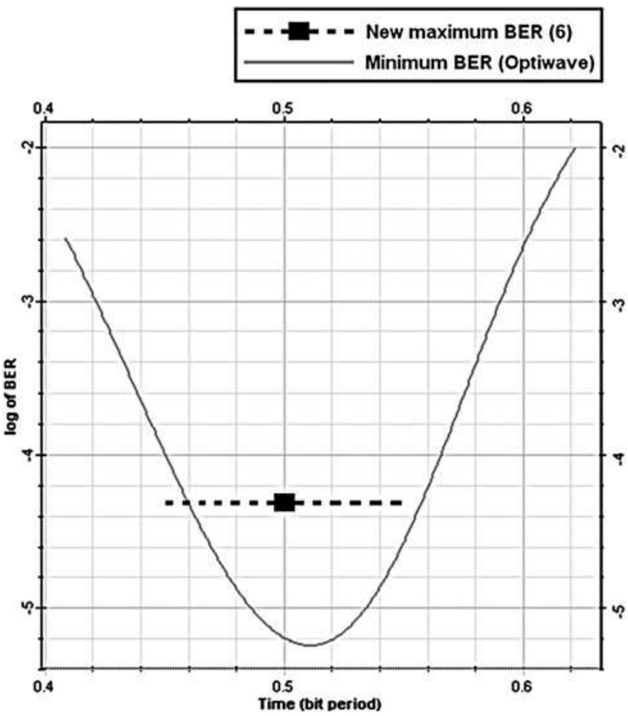

Fig. 6 *Comparison between our new maximum BER and the minimum BER (of Optiwave®), associated with the SSFBG eye diagram decoder of User 1*

6 Conclusions

Many different technologies have been proposed for future generations of PONs. One of them is WDM-PON and another is the coherent OCDMA-PON.

In this paper, a new method is provided to find an upper bound of the error probability as a function of the power contrast ratio *P/C* of the SSFBG code family selected, in a coherent OCDMA-PON system. This new bound will be very useful when a researcher pretends to estimate the maximum BER of an OCDMA system based on the power contrast ratios of a code family. In addition, a new SSFBG power reflection model has been derived and can be useful to understand how to implement perfect sequences in the optical domain. A mathematical property has been provided and should be taken into account in the selection process of SSFBG code families.

7 References

1 Lam, C.: 'Passive optical networks, principles and practice' (Elsevier, 2007)
2 Salehi, J.A., Weiner, A.M., Heritage, J.P.: 'Coherent ultrashort light pulse code division multiple access communication schemes', *J. Lightwave Technol.*, 1990, **8**, (3), pp. 478–491
3 Prucnal, P., Santoro, M., Fan, T.: 'Spread spectrum fiber-optic local area network using optical processing', *IEEE J. Lightwave Technol.*, 1986, **4**, (5), pp. 547–554
4 Santoro, M.A., Prucnal, P.R.: 'Asynchronous fiber optic LAN using CDMA and optical correlation'. Proc. IEEE, 1987, vol. 75, (9), pp. 1336–1338
5 Erdogan, T.: 'Fiber grating spectra', *J. Lightwave Technol.*, 1997, **15**, (8), pp. 1277–1294
6 Teh, P.C., Petropoulos, P., Ibsen, M., Richardson, D.J.: 'A comparative study of the performance of seven- and 63-chip optical code-division multiple-access encoders and decoders based on superstructured fiber Bragg gratings', *J. Lightwave Technol.*, 2001, **9**, pp. 1352–1365
7 Teh, P.C., Ibsen, M., Fu, L.B., Lee, J.H., Yusoff, Z., Richardson, D.J.: 'A 16-channel OCDMA system (4 OCDM x4WDM) based on 16-chip, 20 Gchip/s superstructure fiber Bragg gratings and DFB fiber laser transmitters'. Proc. Optical Fiber Communication Conf. (OFC'2002), Los Angeles, CA, 2002, pp. 600–601
8 Prucnal, P.R.: 'Optical code division multiple access: fundamentals and applications' (CRC Taylor & Francis, 2006)

9 Salihi, J.A., Brackett, C.A.: 'Code division multiple-access technique in optical fiber networks, part I: Fundamental principles and part II: systems performance analysis', *IEEE. Trans. Commun.*, 1989, **37**, pp. 824–842
10 Marhic, M.E.: 'Trends in optical CDMA'. Proc. Multigigabit Fiber Communication (SPIE), 1992, vol 1787, pp. 80–98
11 Huang, J.F., Yen, C.T., Tu, Y.W.: 'Reduction of linear crosstalk over waveguide-grating-based optical CDMA coders/decoders', *J. Opt. Commun. Netw.*, 2010, **2**, (11), pp. 975–983
12 Kitayama, K.I.: 'Code division multiplexing lightwave networks based upon optical code conversion', *IEEE J. Sel. Areas Commun.*, 1998, **16**, pp. 1209–1319
13 Kitayama, K., Wada, N., Sotobayashi, H.: 'Architectural considerations of photonic IP router based upon optical code correlation', *J. Lightwave Technol.*, 2000, **18**, pp. 1834–1844
14 Galli, S., Menendez, R., Narimanov, E., Prucnal, P.: 'A novel method for increasing the spectral efficiency of optical CDMA', *IEEE Trans. Commun.*, 2008, **56**, (12), pp. 2133–2144
15 Okamoto, K.: 'Tutorial review recent progress of integrated optics planar lightwave circuits', *Opt. Quantum Electron.*, 1999, **31**, pp. 107–129
16 Jiang, Z., Seo, D., Yang, S., *et al.*: 'Four-user 10-Gb/s spectrally phase-coded O-CDMA system operating at ∼30 fJ/bit', *IEEE Photon. Tech. Lett.*, 2005, **17**, pp. 705–707
17 Leijtens, X.J.M., Kuhlow, B., Smi, M.K.: 'Arrayed waveguide gratings', available at http://www.alexandria.tue.nl/openaccess/Metis203741.pdf, accessed) April 2013, pp. 1–63
18 Wang, X., Wada, N., Miyazaki, T., Cincotti, G., Kitayama, K.: 'Asynchronous multiuser coherent OCDMA system with code-shift-keying and balanced detection', *IEEE J. Sel. Top. Quantum Electron.*, 2007, **13**, (5), pp. 1463–1470
19 Hamanaka, T., Wang, X., Wada, N., Nishiki, A., Kitayama, K.: 'Ten-user truly asynchronous gigabit OCDMA transmission experiment with a 511-chip SSFBG En/decoder', *J. Lightwave Technol.*, 2006, **24**, (1), pp. 95–102
20 Wang, X., Matsushima, K., Nishiki, A., Wada, N., Kitayama, K.: 'High reflectivity super structured FBG for coherent optical code generation and recognition', *Opt. Express*, 2004, **12**, (22), pp. 5457–5468
21 Smith, E.D.J., Blaikei, R.J., Taylor, D.P.: 'Performance enhancement of spectral-amplitude-coding optical CDMA using pulse-position modulation', *IEEE. Trans. Commun.*, 1998, **46**, pp. 1176–1185
22 Wei, Z., Ghafouri-Shiraz, H., Shalaby, H.M.H.: 'New code families for fiber-Bragg-grating-based spectral-amplitude-coding optical CDMA systems', *IEEE Photon. Technol. Lett.*, 2001, **13**, pp. 890–892
23 Tancevski, T., Rusch, L.A.: 'Impact of the beat noise on the performance of 2-D optical CDMA systems', *IEEE Commun. Lett.*, 2000, **4**, pp. 264–266
24 Sarwate, D., Pursley, M.: 'Crosscorrelation properties of pseudorandom and related sequences', *Proc. IEEE*, 1980, **68**, (5), pp. 593–619
25 Pereira, J., Silva, H.A.: 'A larger subset of pseudo-orthogonal spreading codes for WCDMA, techonline, available at http://www.eetimes.com/design/communications-design/4018072/A-Larger-Subset-of-Pseudo-Orthogonal-Spreading-Codes-for-WCDMA, December 2012
26 Pursley, M.B.: 'Performance evaluation of phase coded spread-spectrum multiple-access communication – Part 1: system analysis', *IEEE Trans. Commun.*, 1977, **25**, (8), pp. 795–799
27 Pereira, J., Silva, H.A.: 'Orthogonal perfect discrete Fourier transform sequences', *IET J. Signal Process.*, 2012, **6**, (2), pp. 107–113
28 Pereira, J., Silva, H.A.: 'Optimal design of perfect DFT sequences', *Phys. Commun.*, 2013, **7**, (1), pp. 92–104
29 Pursley, M.B., Sarwate, D.: 'Performance evaluation of phase coded spread-spectrum multiple-access communication – Part II: code sequence analysis', *IEEE Trans. Commun.*, 1977, **25**, (8), pp. 800–803

doi: 10.1049/iet-spr.2012.0384